JOURNAL OF APPLIED ELECTROCHEMISTRY 25 (1995) 857–863

Influence of zeolite on electrochemical and physicochemical properties of polyethylene oxide solid electrolyte*

N. MUNICHANDRAIAH‡, L. G. SCANLON, R. A. MARSH

Battery Electrochemistry Section, Aero Propulsion and Power Directorate, Wright Laboratory, Wright Patterson AFB OH 45433-7251, USA

B. KUMAR, A. K. SIRCAR

University of Dayton Research Institute, Dayton OH 45469-0170, USA

Received 18 October 1994; revised 19 January 1995

A composite polymer electrolyte of polyethyleneoxide–$LiBF_4$ containing fine particles of zeolite was studied using electrochemical impedance spectroscopy, cyclic voltammetry, differential scanning calorimetry, infrared spectroscopy and scanning electron microscopy. When compared with the polymer electrolyte without zeolite, the specific conductivity of the composite electrolyte film is higher by about two orders of magnitude at room temperature. The increase in specific conductivity is explained as due to increased amorphocity which is reflected in the thermal studies. The nature of the cyclic voltammograms and infrared spectra is discussed.

1. Introduction

There has been a great deal of interest in recent years in the development of high energy rechargeable lithium batteries using a thin film of solid polymer as the electrolyte [1]. Polyethyleneoxide (PEO) has been studied extensively as a polymer-host following the investigations of Wright [2] and Armand [3]. As PEO-based solid polymer electrolytes possess low ionic conductivity which is not suitable for practical applications, several ways of modifying this polymer in order to enhance its conductivity have been studied. Addition of inert fine particles such as alumina, lithiated alumina, Nasicon, silica etc., [4–8] resulted in enhancement of the conductivity to some extent. In the present studies, the influence of fine particles of zeolite on physicochemical and electrochemical properties of PEO–$LiBF_4$ electrolyte has been investigated.

2. Experimental details

The polymer electrolyte films were prepared by solution casting. The required quantity of PEO of molecular weight 300 000 (Union Carbide) was dissolved in AR grade acetonitrile (Aldrich) under stirring. An appropriate quantity of dry $LiBF_4$ (Aldrich) was also dissolved following which the solution was continuously stirred for about 24 h. The O:Li ratio was maintained at 8:1 in the PEO–$LiBF_4$ complex. The required amount of zeolite (Aldrich) of particle size 5 μm was added to the complex solution whenever required. Ensuring complete dissolution and uniform dispersion of the zeolite particles in the solution, films were cast on PTFE covered glass plates. The solvent was allowed to evaporate slowly at room temperature which was followed by drying at 80 °C under vacuum for about 24 h, before the films (thickness 100–150 μm) were transferred and used in a helium filled dry box (oxygen and water < 30 ppm).

The electrochemical studies were carried out by constructing SS/SPE/SS and (SS)Li/SPE/Li(SS) [where SS refers to stainless steel and SPE refers to solid polymer electrolyte] symmetrical cells in PTFE holders. The cell was mounted in an air-tight glass container, which was subsequently evacuated. The glass container was heated to the required temperature and maintained within ±1 °C by using a heating tape and a temperature controller.

Electrochemical impedance measurements were carried out using PAR(EG&G) instrument model 368 in the frequency range from 0.1 Hz to 100 kHz. Cyclic voltammograms were recorded using a PAR (EG&G) instrument model 273A. The polymer electrolyte samples were subjected to differential scanning calorimetry (DSC) using a TA Instruments model 910 and system controller 2100. Infrared spectra were recorded for very thin films of the polymer electrolyte using a Nicolet FTIR spectroscope. The microstructures of the films were evaluated using an International Scientific Instruments model SIIIA scanning electron microscope.

* Part of this work was presented at the Electrochemical Society Meeting, Honolulu, Hawai (May 1993).

‡ On leave from Department of Inorganic and Physical Chemistry, Indian Institute of Science, Bangalore-560 012, India.

0021-891X © 1995 Chapman & Hall

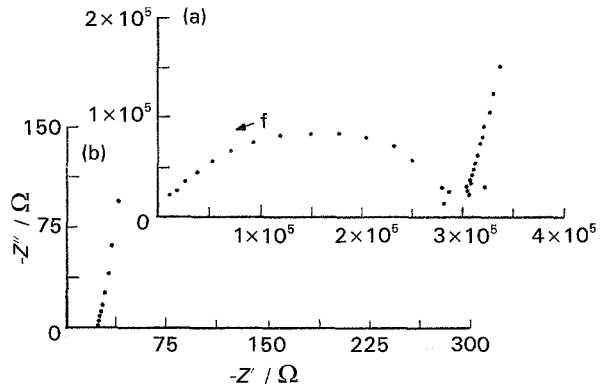

Fig. 1. Nyquist plots of SS/$(PEO)_8LiBF_4$, 20 wt % zeolite/SS at (a) 26 °C and (b) 76 °C. Film thickness 150 μm; crosssection area 1.1 cm^2.

3. Results and discussion

3.1. *Conductivity studies*

The specific conductivity, σ, of the polymer electrolyte film was calculated from the impedance diagram of the SS/SPE/SS symmetrical cell. A typical Nyquist plot of the impedance data is shown in Fig. 1. The presence of a semicircle followed by a linear spike at low frequency range at ambient temperatures, as shown in Fig. 1(a), is similar to what is reported in the literature [9]. In the electrochemical equivalent circuit, the semicircle is attributed to a parallel combination of the geometric capacitance and the resistance of the polymer electrolyte film. The σ of the SPE was calculated from the intercept of the semicircle on the real axis of the Nyquist plot. When the measurements were carried out at higher temperatures, the semicircle did not appear (Fig. 1(b)). As the resistance of the polymer film decreased with increase in temperature, the frequency range required for the appearance of the semicircle occurred higher than 100 kHz, which was a limitation of the measuring instrument in the present studies. In such a case, σ was calculated from the intercept of the linear spike.

The σ of the polymer electrolyte containing different compositions of zeolite in the temperature range 20–100 °C is shown in Fig. 2. There is a rapid increase in σ with increase in temperature up to about 70 °C, and above this temperature, the increase is marginal. This transition temperature corresponds to the melting point of the polymer electrolyte. At a particular temperature, σ increases with increase in concentration, to about 29 wt % of zeolite in the polymer electrolyte. The σ at 20 °C, for example, increases from 10^{-9} S cm^{-1} (absence of zeolite) to about 10^{-7} S cm^{-1} when the concentration of zeolite is 29 wt %. Further increase of zeolite concentration results in a drastic decrease of σ. These results may be explained as follows. PEO possesses partial crystallinity at temperatures less than about 70 °C, and the ionic conduction takes place essentially in the amorphous phase of the electrolyte [10]. Owing to the presence of zeolite particles, the crystallinity of the polymer electrolyte decreases as inferred from the DSC studies (cf. Section 3.3), resulting in increased conductivity. Another explanation is that the ionic conduction may be faster at the boundary of zeolite particle/polymer medium, similar to the effect of inert particles (e.g., Al_2O_3) in inorganic ionic conductors such as LiI [11]. At 38 wt % of zeolite in the polymer electrolyte, however, contact among zeolite particles becomes dominant leading to decreased conductivity.

3.2. *Cyclic voltammetric studies*

Cyclic voltammograms of (SS)Li/SPE/Li(SS) symmetrical cells were recorded. As these studies were intended to qualitatively examine the influence of zeolite, the voltammograms were recorded without using a reference electrode, similar to the studies reported in the literature [12, 13]. The problems associated with introducing a reference electrode into a thin film of polymer electrolyte were recently reported [14]. A cyclic voltammogram of the cell with PEO electrolyte not containing zeolite is shown in Fig. 3. A close observation of the curve reveals the existence of two anodic peaks and two cathodic peaks, instead of a single peak, which is expected if the electrode reaction proceeds as a simple electron transfer process:

$$Li^+ + e^- = Li \qquad (1)$$

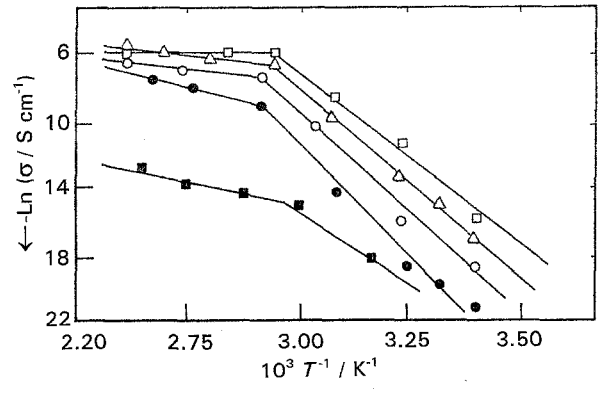

Fig. 2. Specific conductivity (σ) as a function of inverse temperature for $(PEO)_8LiBF_4$ electrolytes containing different concentrations of zeolite: (●) nil, (○) 8, (△) 20, (□) 29 and (■) 38 wt %.

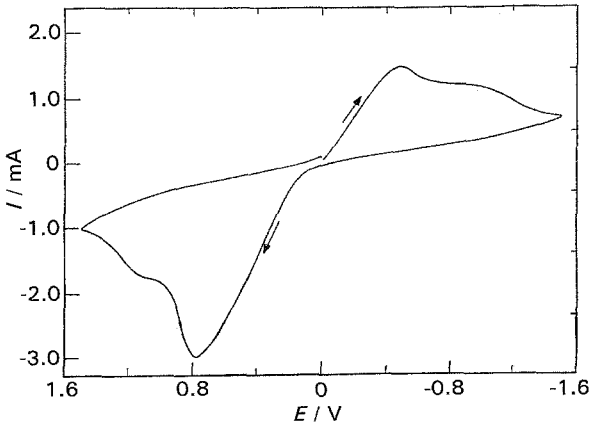

Fig. 3. Cyclic voltammogram of Li/$(PEO)_8LiBF_4$/Li cell at a scan rate of 5 mV s^{-1} and 80 °C. Film thickness 110 μm; lithium electrode area 0.65 cm^2.

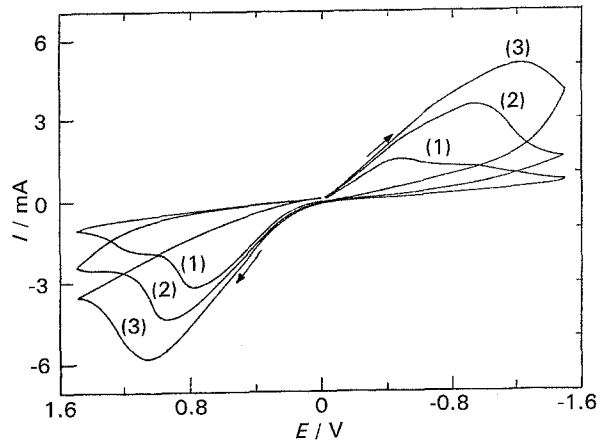

Fig. 4. Cyclic voltammogram of Li/$(PEO)_8LiBF_4$/Li cell at 80 °C. Scan rates: (a) 5, (b) 10 and (c) 20 mV s^{-1}. Film thickness 110 μm; lithium electrode area 0.65 cm^2.

The voltammograms recorded at several scan rates are shown in Fig. 4. By increasing the scan rate, the two cathodic peaks merge, resulting in a broad peak. The presence of more than one peak in the anodic or cathodic sweep is rarely reported [15]. When a Pt substrate was used, the second current peak was attributed to the formation of Pt–Li alloy. In the present studies, however, such a possibility does not exist, since lithium metal was used as the substrate for plating and stripping of lithium. The following explanations are considered for additional peaks:

(i) Although sufficient care had been taken to exclude water during the preparation of the electrolyte film and the assembly of the cell, it is likely that the electrolyte contained a trace quantity of water. The electrochemical oxidation and reduction processes of water molecules on lithium might be responsible for the appearance of additional anodic and cathodic peaks.

(ii) The anion of the salt used in the present work viz. BF_4^- may undergo reduction as the following reaction is feasible in aqueous medium [16].

$$BF_4^- + 3e^- = B + 4F^- \qquad E^\circ = -1.04\,V \quad (2)$$

The additional voltammetric peaks may be attributed to the reactions involving BF_4^- anion. The kinetic barrier, however, is very large and only a film containing products like LiF is likely to be formed at the Li surface.

(iii) The lithium surface is usually believed to be covered with primary and secondary passive layers [17]. While the primary passive layer is considered to allow Reaction 1 to proceed through it, the secondary passive layer, the coverage of which is less than unity, can change the mechanism of the reaction. Reaction 1 can be considered as taking place at two different potentials across the primary and secondary passive layers.

The cyclic voltammograms of symmetrical cells with the electrolyte samples containing several concentrations of zeolite are shown in Fig. 5. The trace for the electrolyte film containing 8 wt % of zeolite (curve 2 of Fig. 5) resembles curve 1, which is for the electrolyte not containing zeolite. On further increasing the zeolite concentration, however, the first cathodic peak current decreased and the second cathodic peak current increased (curves 3, 4 and 5 of Fig. 5). The dependence of cathodic peak currents on the concentration of zeolite is shown in Fig. 6. The zeolite particles thus retard and catalyse the reactions, corresponding to the first and second cathodic peaks, respectively. Another interesting aspect of these studies is that the cathodic peak currents decreased with an increase in scan rate, as shown in Fig. 7 for the electrolyte containing 20% zeolite. This is in contrast to a normal diffusion controlled

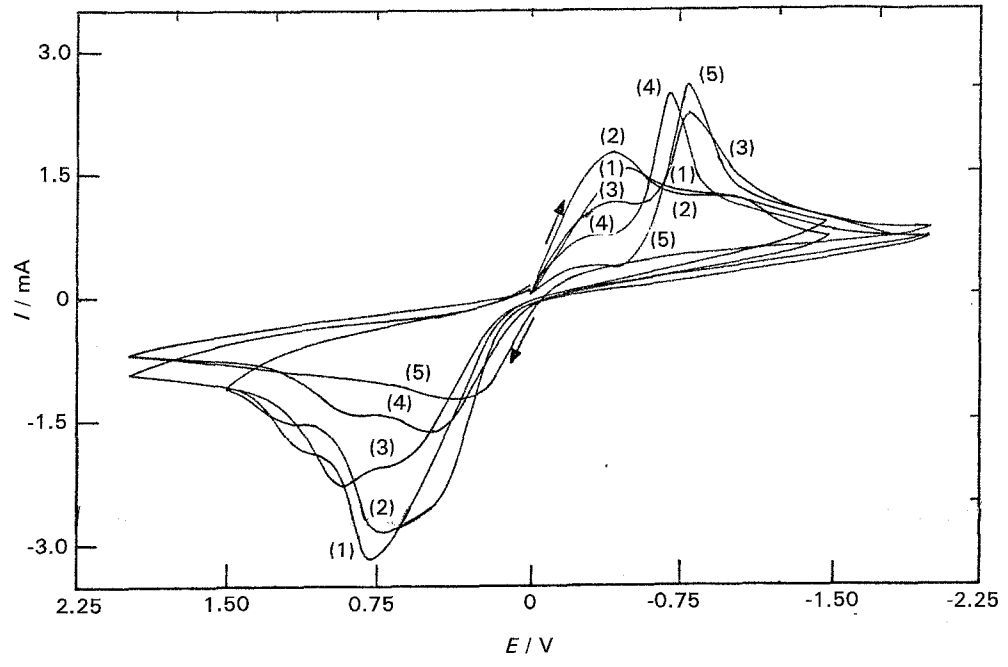

Fig. 5. Cyclic voltammograms of Li/$(PEO)_8LiBF_4$/Li at 80 °C. Concentration of zeolite in the polymer electrolyte: (1) 0, (2) 8, (3) 14, (4) 20 and (5) 24 wt %. Film thickness 110 μm; lithium electrode area 0.65 cm^2.

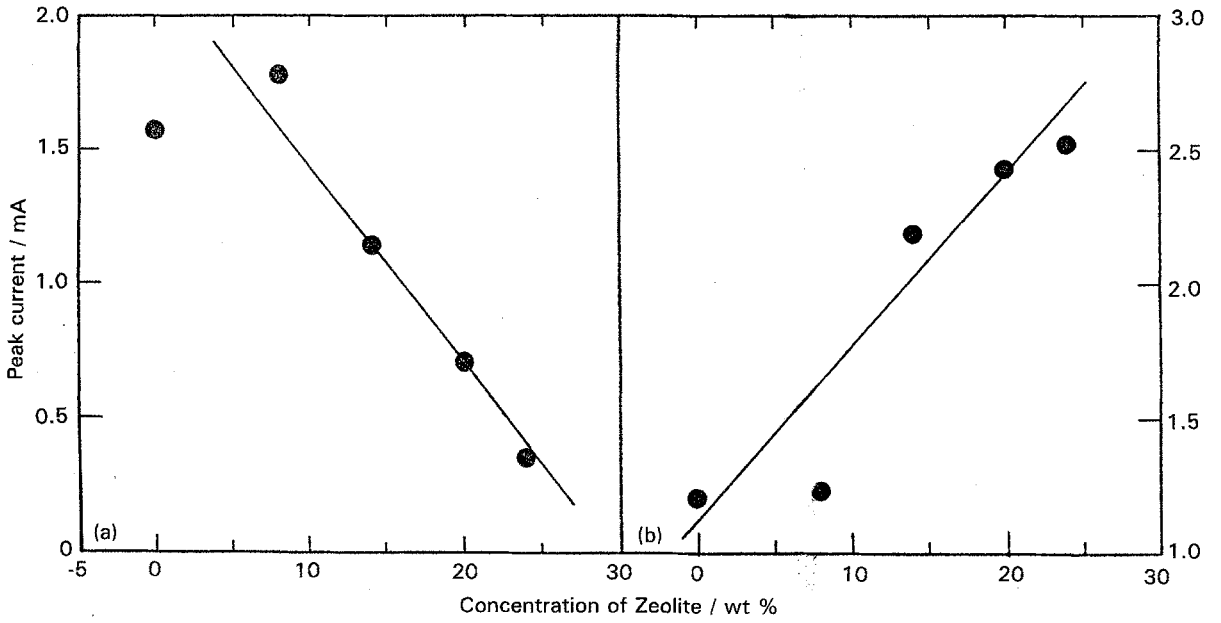

Fig. 6. The cathodic peak current of cyclic voltammogram as a function of zeolite concentration. (a) First cathodic peak; (b) second cathodic peak. Temperature 80 °C; film thickness 110 μm; lithium electrode area 0.65 cm^2.

voltammogram in which the peak current should increase linearly with the square root of scan rate. The anodic part of the voltammogram (Fig. 5) shows a gradual decrease in the peak current with increase in zeolite concentration, thus suggesting that the zeolite particles present in the polymer electrolyte retard the anodic stripping of Li metal to some extent.

The appearance of the second cathodic peak can also be attributed to the reduction of Na^+ present in the polymer film. The presence of Na^+ may be thought to originate from the exchange of Li^+ in the polymer electrolyte with Na^+ of the zeolite. However, the possibilities for Li^+/Na^+ exchange are remote, since the smaller ionic size of Li^+ does not favour the exchange of a larger ion (i.e., Na^+) in zeolite [18]. Moreover, PEO electrolyte may enter the zeolite pores. While the first cathodic peak can be considered due to the reduction of Li^+ ion from the SPE, the second peak can be attributed to the reduction of Li^+ ion present together with PEO in the zeolite pores. This possibility exists when zeolite is present in the SPE, in addition to the several other possibilities considered above. More experimental work is required to throw light on this problem.

3.3. *Differential scanning calorimetry*

Differential scanning calorimetric behaviour of $(PEO)_8LiBF_4$ complexes containing several concentrations of zeolite were recorded at a scan rate of

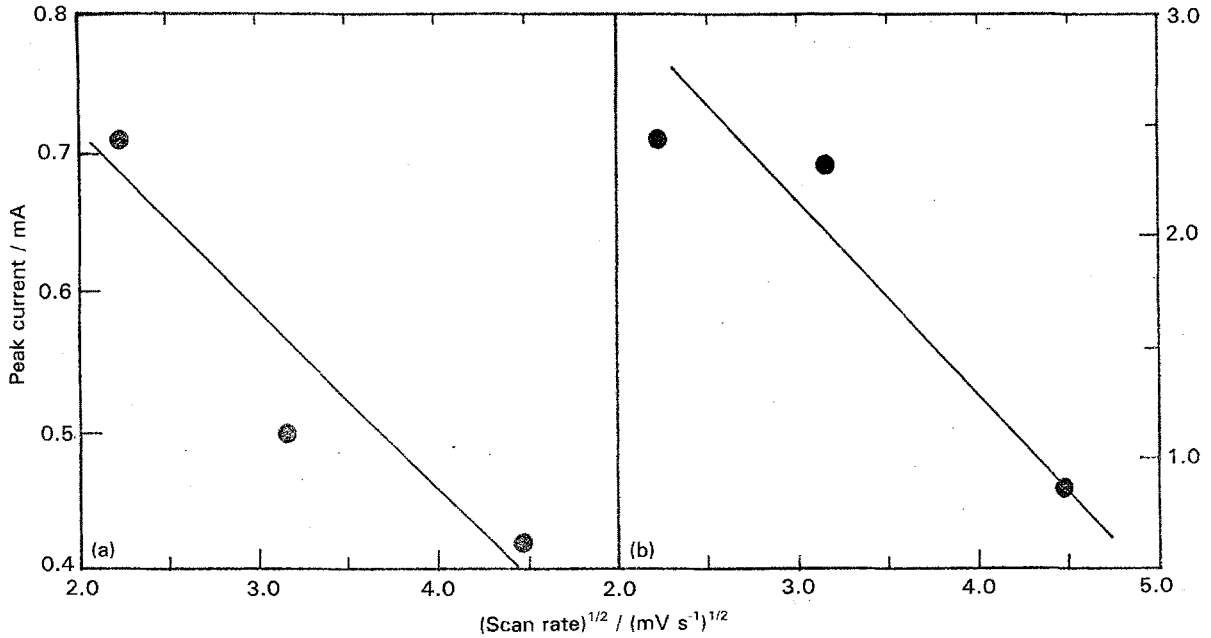

Fig. 7. The dependence of cathodic peak current of Li/$(PEO)_8LiBF_4$ + 20 wt % zeolite/Li on square root of scan rate. (a) First cathodic peak; (b) second cathodic peak. Temperature 80 °C; film thickness 110 μm; lithium electrode area 0.65 cm^2.

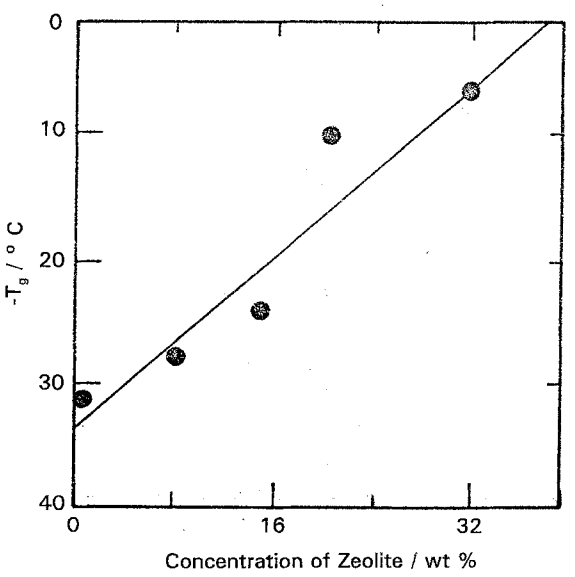

Fig. 8. Glass transition temperature (T_g) of $(PEO)_8LiBF_4$ against zeolite concentration.

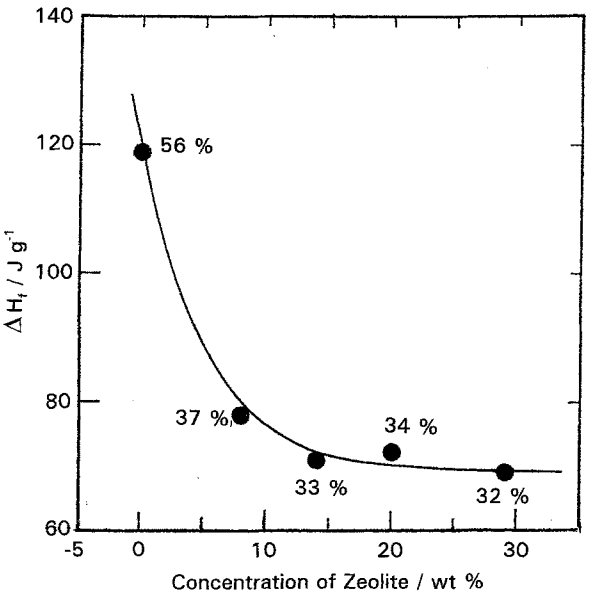

Fig. 9. Variation of heat of fusion (ΔH_f) of $(PEO)_8LiBF_4$ as a function of zeolite concentration. The number shown on each point is the degree of crystallinity.

20 °min^{-1} between −100 °C and 100 °C. The DSC trace recorded starting from −100 °C did not show a clear glass transition region. When recorded after annealing the sample at 100 °C for 2 min followed by cooling to −100 °C at a rate of 20 °min^{-1}, a clear glass transition (T_g) region resulted. The T_g values as a function of zeolite concentration are shown in Fig. 8.

The DSC results can be discussed on the basis of the PEO–$LiBF_4$ system phase diagram reported in the literature [19, 20]. At the stoichiometry of $(PEO)_8LiBF_4$, there are two crystalline phases coexisting at low temperatures. By annealing at 100 °C and subsequent cooling to −100 °C, crystallization of PEO was incomplete and therefore the glass transition was clearly noticed. The glass transition temperature (T_g) of $(PEO)_8LiBF_4$ was −31 °C (Fig. 8), which is higher than the T_g of pure PEO (−60 °C). This increase in T_g is due to complexation of PEO with $LiBF_4$. Owing to the presence of zeolite, the T_g further increased and was approximately −6 °C when the zeolite concentration was 32 wt %. The T_g value generally depends on the thermal history of the sample. Since all electrolyte samples were subjected to identical heat treatment in the present studies, the increase in T_g is attributed to the presence of zeolite. The increase in T_g reflects an increase in salt concentration from dissolution of the stoichiometric complex in the amorphous phase, and/or a specific interaction between PEO and zeolite. The latter aspect was confirmed by spectroscopic studies (cf. Section 3.4).

Using the DSC scans recorded prior to annealing, the heat of fusion, ΔH_f, was calculated from the endothermic melting transition, and is shown as a function of zeolite concentration in Fig. 9. There is a sudden decrease in ΔH_f due to the first addition of zeolite, followed by a gradual decrease on further increasing its concentration. This suggests that the crystallinity of the polymer electrolyte reduces due to the presence of zeolite particles. Taking $\Delta H_f = 214\,J\,g^{-1}$ [21] for a completely crystalline PEO, the degree of crystallinity was calculated and is shown in Fig. 9. The increase in amorphous content of the polymer complex owing to the presence of zeolite particles was essentially responsible for the increase in σ, as discussed in Section 3.1.

3.4. *Infrared spectroscopy*

The middle IR spectra recorded for PEO and PEO

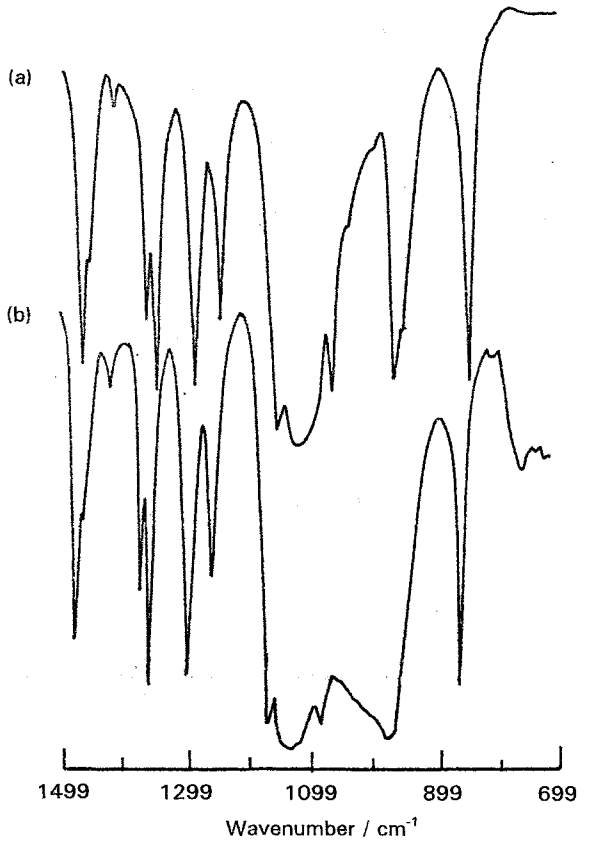

Fig. 10. Infrared spectra of films (a) PEO and (b) PEO containing 10 wt % zeolite.

containing zeolite are shown in Fig. 10. The spectrum of PEO is identical to that reported in the literature [22]. The strong infrared bands at 844 and 958 cm^{-1} are for CH_2 rocking modes. The band at about 1147 cm^{-1} is for CC or COC stretching modes. The bands appearing at 1244, 1358 and 1473 cm^{-1} are for CH_2 twisting, wagging and bending modes, respectively. The spectrum of PEO containing zeolite (Fig. 10(b)) resembles that of PEO except that the bands merge and become broad in the region between 950 and 1150 cm^{-1}. This part of the infrared spectrum is similar to that of PEO complexed with an ionic salt [22]. This suggests the existence of a chemical interaction between PEO and zeolite particles. The absence of an infrared band at about 920 cm^{-1} indicates that there is no complex formation between PEO and Na^+, if the latter is assumed to be present as a soluble impurity from zeolite. It is known [23] that PEO forms molecular complexes with non-ionic compounds. The pattern of the infrared spectrum between 950 and 1150 cm^{-1} is likely to be due to the formation of a molecular complex between PEO and zeolite particles.

3.5. *SEM studies*

The SEM micrographs of PEO and PEO containing zeolite are shown in Fig. 11. There is a uniform distribution of zeolite particles. The crystal size of PEO reduces and the grain boundaries disappear due to the presence of zeolite. These results provide supporting evidence for decreased PEO crystallinity in the presence of zeolite particles.

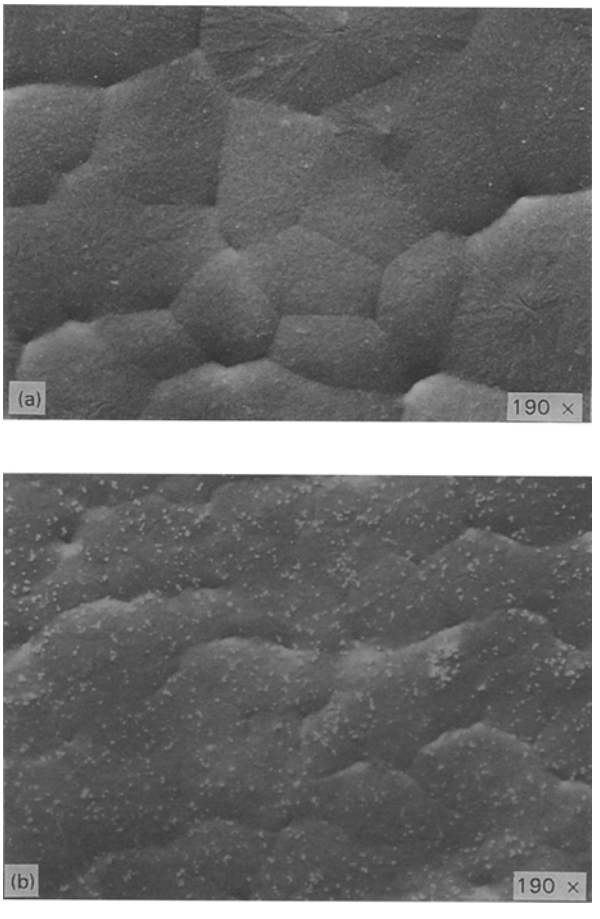

Fig. 11. The SEM micrographs of films (a) PEO and (b) PEO containing 10 wt % zeolite.

4. Conclusions

It is shown that fine particles of zeolite dispersed in PEO–$LiBF_4$ electrolyte film impart some unusual properties, in particular to the cyclic voltammetric response. Even though the conclusions from these studies are qualitative in nature, the results are important in view of the present trend in composite polymer electrolyte studies. Although the increase in σ due to the presence of zeolite particles is not substantial, there is a clear indication of increase in the amorphous phase of the polymer electrolyte. The infrared spectra suggest the formation of a molecular complex between PEO and zeolite particles.

Acknowledgement

One of the authors (NM) is grateful to the National Research Council of USA for a Research Associateship. John Leonard is thanked for taking the SEM micrographs.

References

[1] M. Gauthier, A. Belanger, B. Kapfer, G. Vassort and M. Armand in 'Polymer Electrolyte Reviews – 2' (edited by J. R. MacCallum and C. A. Vincent), Elsevier, Oxford/London (1989) p. 285.
[2] P. V. Wright, *Brit. Polym. J.* **7** (1975) 319.
[3] M. B. Armand, J. M. Chabagno and M. J. Duclot, in 'Fast Ion Transport in Solids', (edited by P. Vashishta, J. N. Mundy and G. K. Shenoy), North-Holland, Amsterdam (1979) p. 131.
[4] F. Capuano, F. Croce and B. Scrosati, *J. Power Sources* **37** (1992) 369.
[5] F. Capuano, F. Croce and B. Scrosati, *J. Electrochem. Soc.* **138** (1991) 1918.
[6] F. Croce, F. Capuano, A. Selvaggi, B. Scrosati and G. Scibona, *J. Power Sources* **32** (1990) 381.
[7] J. Przyluski, K. Such, H. Wycislik, W. Wieczorek and Z. Florianczyk, *Syn. Met.* **35** (1990) 241.
[8] J. Plocharski and W. Wieczorek, *Solid State Ionics* **28–30** (1988) 979.
[9] P. G. Bruce in 'Polymer Electrolyte Reviews – 1' (edited by J. R. MacCallum and C. A. Vincent) Elsevier, London/New York (1987) p. 237.
[10] C. Berthier, W. Gorecki, M. Minier, A. B. Armand, J. M. Chabagno and P. Rigaud, *Solid State Ionics* **11** (1983) 91.
[11] C. Liang, *J. Electrochem. Soc.* **120** (1973) 1289.
[12] R. Hug, R. Koksbang, P. E. Tonder and G. C. Farrington, in 'Proceedings of the Symposium on Primary and Secondary Lithium Batteries', (edited by K. M. Abraham and M. Salomon), Electrochemical Society, **91-3** (1991), p. 147.
[13] N. Munichandraiah, L. G. Scanlon, R. A. Marsh, B. Kumar and A. K. Sircar, *J. Appl. Electrochem.* **24** (1994) 1066.
[14] N. Munichandraiah, L. G. Scanlon, R. A. Marsh, B. Kumar and A. K. Sircar, *J. Electroanal. Chem.* **379** (1994) 495.
[15] B. Scrosati, in 'Polymer Electrolyte Reviews – 1', (edited by J. R. MacCallum and C. A. Vincent), Elsevier, London/New York (1987), p. 315.
[16] J. Lurie, 'Handbook of Analytical Chemistry', Mir Publishers, Moscow (1975), p. 301.

[17] E. Peled, in 'Lithium Batteries', (edited by J.-P. Gabano) Academic Press, London/New York (1983), p. 43.
[18] R. M. Barrer, in 'Natural Zeolites: Occurrence, Properties, Use', (edited by L. B. Sand and F. A. Mumpton), Pergamon Press, Oxford (1978), p. 385.
[19] M. Z. A. Munshi and B. B. Owens, *Appl. Phys. Comm.* **6** (1987) 279.
[20] S. M. Zahurak, M. L. Kaplan, E. A. Rietman, D. W. Murphy and R. J. Cava, *Macromolecules* **21** (1988) 654.
[21] X. Li and S. L. Hsu, *J. Polym. Sci. Polym. Phys. Ed.* **22** (1984) 1331.
[22] B. L. Papke, M. A. Ratner and D. F. Schriver, *J. Phys. Chem. Solids* **42** (1981) 493.
[23] E. Delaiti, J. J. Point, P. Damman and M. Dosiere, *Macromolecules* **25** (1992) 4768.